Relative Trajectories of Objects Ejected from a Near Satellite

GILBERT C. KNOLLMAN* AND BERRY O. PYRON†

Georgia Institute of Technology, Atlanta, Ga.

An unpowered, unconstrained object is considered to be ejected impulsively with low speed from a satellite in circular orbit. The ejection velocity vector has an arbitrary direction within the satellite's orbital plane. Equations are developed describing the object's motion relative to a frame of reference centered on the satellite for the general case that atmospheric drag acts on the object. Typical trajectories (obtained on an analog computer) are illustrated by plots applying to two objects having different values of ballistic drag parameter and to both low-speed ejection and zero-speed release. The effects upon trajectory shape of varying altitude, ejection speed and angle, and drag parameter are indicated, and particular aspects of the trajectories are discussed. In addition, the simplified case of no drag is examined analytically. Approximate equations are developed for the trajectory of the object in that case, the shape of the trajectory with various ejection angles is discussed, and orbital parameters are derived.

ALTHOUGH the orbital motion of individual satellites has been studied extensively, both with and without the effect of atmospheric drag force included, less attention seems to have been given to the motion of orbital bodies relative to one another. In particular, the authors have not found discussed in the literature certain noteworthy features of the behavior of an object ejected from an orbiting satellite, and yet the separation of bodies with small relative speed occurs in a variety of orbital operations. Satellite instrument capsules commonly are separated from their rocket carriers by means of small impulsive forces. Casings and other no-longer-wanted parts are thrust away. Two or more satellites may be placed in orbit by a single carrier and then separated from one another. Furthermore, one may envision that, in future operations around manned satellite stations or vehicles, space-suited men, tools, and other objects will become separated, accidentally or intentionally, from the "parent" craft. These and other instances suggest that the motion of orbital bodies, subsequent to their separation with modest relative speed, is of interest. In addition, the relative motion of orbiting objects is of importance in problems relating to satellite rendezvous and intercept.[1−10]

This paper is concerned with the behavior of an unpowered object ejected from a satellite in circular orbit about the earth and thereafter acted upon only by the earth's gravitational field and atmospheric drag force. For convenience, only ejection within the plane of the satellite orbit is examined. The object is assumed to be ejected impulsively with a speed relative to the satellite which is small compared with the satellite's orbital speed; the ejection velocity vector makes an arbitrary angle with the orbital velocity vector. An ideal satellite is selected as the origin of the frame of reference for studying the object's motion; this ideal satellite undergoes no drag force and no reaction force to the impulsive kick that ejects the body.‡ Spherical symmetry is assumed for the earth's gravitational field and for its atmosphere. Minor effects upon the body's behavior, such as interaction with the earth's magnetic field and with the gravitational fields of bodies other than the earth, are neglected.

Received by ARS June 4, 1962; revision received November 6, 1962.

* Research Scientist, Research Laboratories, Lockheed Missiles and Space Co., Palo Alto, Calif.; formerly Research Physicist, Engineering Experiment Station.

† Research Physicist, Engineering Experiment Station.

‡ The stipulation of no reaction force may be taken to imply that the body's mass is negligibly small compared with that of the satellite.

Geometrical Problem Model

Figure 1 depicts the interrelationships among the three two-dimensional Cartesian coordinate systems to be used in describing the problem. The x_1, y_1 system is nonrotating and has its origin at the earth's center, whereas x_2, y_2 has the same origin but rotates with the constant angular speed ω_C of the ideal, no-drag satellite. The x_3,y_3 system has its origin in the ideal satellite with the x_3 axis along the satellite's velocity vector of magnitude V_C and the y_3 axis forming an angle β with the y_1 axis.

Equations of Relative Motion

The object is ejected at an angle φ with respect to the x_3 axis and with a speed V_R relative to the satellite; the satellite is assumed to be in a circular orbit of radius R_C. After ejection, the object moves in a quasi-elliptic orbit of decreasing eccentricity which eventually degenerates into an approximately circular orbit and thereafter into a spiral tightening about the earth. This degeneration is brought about by the continuous dissipation of energy caused by atmospheric drag. With respect to the satellite-fixed coordinate frame, the launched object at any time has position x_3,y_3.

The authors are primarily concerned with the ejected object's motion relative to the x_3,y_3 coordinate system, that is, with the motion as seen by an observer riding on a satellite with his feet always oriented toward and his head away from the center of the earth. However, occasional mention is made of the object's motion relative to the geocentric system x_1,y_1. In the interest of clarity, then, the term "trajectory" is restricted to mean the object's path relative to the x_3,y_3 frame, and the term "orbit" is used only in reference to its motion relative to x_1,y_1.

Equations of motion for the ejected object relative to the nonrotating inertial frame shown in Fig. 1 can be written in the well-known form

$$\ddot{x}_1 + (\mu/r_1^3)x_1 + B\rho\dot{x}_1(\dot{x}_1^2 + \dot{y}_1^2)^{1/2} = 0 \qquad (1)$$

$$\ddot{y}_1 + (\mu/r_1^3)y_1 + B\rho\dot{y}_1(\dot{x}_1^2 + \dot{y}_1^2)^{1/2} = 0 \qquad (2)$$

in which μ is the product of the universal gravitational constant times the sum of object mass and earth mass, ρ is the air density at the position x_1, y_1, and r_1 is the instantaneous radial distance of the ejected body from the center of the earth given by

$$r_1 = (x_1^2 + y_1^2)^{1/2} \qquad (3)$$

The ballistic drag parameter B is defined as

$$B = AC_D/2m \quad (4)$$

where m and A are, respectively, the mass and effective drag area§ of the ejected object, and C_D represents the (dimensionless) aerodynamic drag coefficient.

Under the orthogonal transformation in β appropriate for a rotation of axes, Eqs. (1) and (2) transform to describe the motion relative to the x_2,y_2 frame. Differential equations relative to the x_3,y_3 frame are finally obtained by substituting

$$x_2 = x_3 \qquad y_2 = y_3 + R_C \quad (5)$$

To reduce the result to a form more suitable for solution by analog-computational methods, one makes the change of variable $\beta = \omega_C t$ and introduces the relationship $\mu = \omega_C{}^2 R_C{}^3$, which applies for circular orbits.‖ The satellite angular speed in orbit is given by

$$\omega_C = \dot{\beta} = V_C/R_C \quad (6)$$

Designating by primes derivatives with respect to β, one obtains

$$x_3'' + 2y_3' - x_3[1 - (R_C/r_3)^2] + (B\rho V_3/\omega_C) \times (x_3' + y_3 + R_C) = 0 \quad (7)$$

$$y_3'' - 2x_3' - (y_3 + R_C)[1 - (R_C/r_3)^2] + (B\rho V_3/\omega_C)(y_3' - x_3) = 0 \quad (8)$$

wherein the object speed V_3 with respect to the x_3,y_3 coordinate system is

$$V_3 = \omega_C[(x_3' + y_3 + R_C)^2 + (y_3' - x_3)^2]^{1/2} \quad (9)$$

and

$$r_3 = [x_3{}^2 + (y_3 + R_C)^2]^{1/2} \quad (10)$$

For relative separations between object and satellite which are small compared with the radius of the orbit (which, in turn, implies ejection speeds small compared to the orbital speed), Eq. (10) is approximated by two terms in its binomial expansion. Introducing the result into (7) and (8) yields

$$x_3'' + 2y_3' - \tfrac{3}{2}(x_3/R_C{}^2)(x_3{}^2 + y_3{}^2 + 2y_3R_C) + (B\rho V_3/\omega_C)(x_3' + y_3 + R_C) = 0 \quad (11)$$

$$y_3'' - 2x_3' - \tfrac{3}{2}[(y_3 + R_C)/R_C{}^2](x_3{}^2 + y_3{}^2 + 2y_3R_C) + (B\rho V_3/\omega_C)(y_3' - x_3) = 0 \quad (12)$$

These equations provide the desired description of the ejected object's motion relative to the x_3,y_3 frame centered on the ideal satellite, with the effect of air drag included. Initial conditions imposed on (11) and (12) are

$$x_3(0) = y_3(0) = 0 \quad (13)$$

$$x_3'(0) = \eta R_C \cos\varphi \quad (14)$$

$$y_3'(0) = \eta R_C \sin\varphi \quad (15)$$

in which

$$\eta = V_R/V_C \quad (16)$$

is the ratio of relative ejection speed to satellite orbital speed, and φ is the angle of ejection with respect to the satellite's velocity vector (i.e., the x_3 axis).

§ The effective drag area of an object depends upon its geometrical shape as well as its orientation relative to the air stream. A nonconcave object randomly tumbling throughout its motion in the atmosphere has an effective drag area that is one fourth its total surface area.

‖ Although the quantity μ in Eqs. (1) and (2) refers to the ejected object, it may be regarded as also applying to the satellite if both the satellite mass and the mass of the ejected object are small in comparison with the earth's mass.

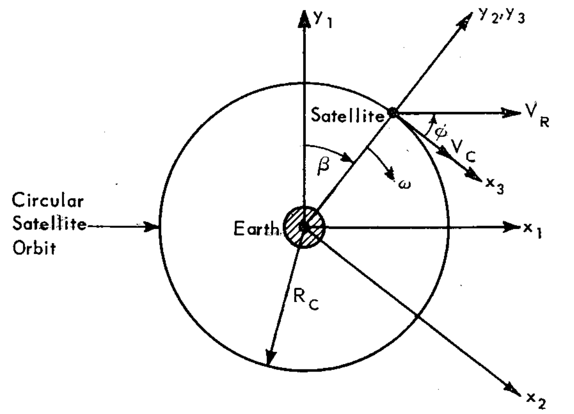

Fig. 1 Rectangular coordinate systems

Special Case: Zero Drag

As will be shown later, the relative trajectory followed by an ejected body in the atmosphere can be regarded in first approximation as comprising a superposition of the forward displacement occasioned by air drag upon the path that would otherwise prevail. For this reason, one first studies the ejection problem with atmospheric drag effects suppressed, which may be accomplished by taking $B = 0$. This simplified case provides an insight into the more complex case where drag is included by illustrating several characteristic features that the latter also displays.

This special case of zero drag approximates the more complex case at great altitudes. Moreover, zero drag trajectories closely approximate for a considerable time those that prevail in the event that the satellite, as well as the object, undergoes drag and that both have the same value of drag parameter and therefore experience nearly the same drag acceleration so long as they are at nearly the same altitude.

In the absence of aerodynamic drag, an object ejected with small relative speed from a satellite in circular orbit will thereafter follow an elliptic orbit of very small eccentricity having a focus at the earth's center; this orbit lies everywhere close to the orbit of the satellite. In the circumstance that satellite and ejected body have unequal periods of revolution about the earth, the one having the shorter period will creep ahead of the other in orbital position, and this steady advancement soon will produce substantial separations between the bodies.# On the other hand, for the particular case that satellite and ejected object have equal periods of revolution, they will continue indefinitely (under the stated assumptions) to orbit the earth "in step." After each revolution, the ejected body will return to the satellite's position with its initial relative velocity and hence will again and again retrace the same "closed" trajectory in the x_3,y_3 coordinate system.

Elliptic Orbit Parameters

The ejected object's elliptic orbit with respect to the x_1,y_1 reference frame is identified completely in the present problem by determining three orbit parameters: the semimajor axis length a, eccentricity ϵ, and angle θ between the lines joining the earth's center with the point of ejection and with the perigee. (In the case of nonzero drag, the forementioned parameters apply approximately to the instantaneous elliptical orbit of the ejected body at the moment of launch.)

At the instant of launch, the ejected object's velocity with respect to the x_1,y_1 coordinate system is the resultant of the

For this special case of zero drag and under the idealized conditions of this analysis, the satellite and ejected body once again will be in proximity after some great number of revolutions, but the authors are not concerned here with such long time periods.

velocities having magnitudes V_R and V_C (see Fig. 1). Designating the object's actual speed at launch by V_B and using the law of cosines, one finds that

$$(V_B/V_C)^2 = 1 + \eta^2 + 2\eta \cos\varphi \tag{17}$$

Since V_B is the speed of a body in an elliptic orbit and at a distance R_C from the origin of a coordinate system centered at a focus, the following relation can be written:

$$V_B^2 = (\mu/R_C)(2 - R_C/a) \tag{18}$$

which applies for any mass moving solely under the influence of an inverse-square-law central-force field. With the satellite speed V_C given by $V_C^2 = \mu/R_C$, Eq. (18) becomes $(V_B/V_C)^2 = 2 - R_C/a$. Introducing this result into Eq. (17) and then solving for the semimajor axis length, one obtains

$$a = R_C[1 - \eta^2 - 2\eta \cos\varphi]^{-1} \tag{19}$$

To determine the eccentricity ϵ of the elliptic orbit, one notes that at the instant of ejection the object's tangential component of actual speed, $V_R \cos\varphi + V_C$, must equal that appropriate for an object in an elliptic orbit and at a radial distance R_C from the origin of a focus-centered coordinate system. Hence,

$$V_C^2(1 + \eta \cos\varphi)^2 = \mu a(1 - \epsilon^2)/R_C^2 \tag{20}$$

When Eq. (20) is solved for ϵ and Eq. (19) is substituted for a the result is

$$\epsilon = \eta[\eta^2 \cos^2\varphi + 2\eta(1 + \cos^2\varphi) \cos\varphi + (1 + 3 \cos^2\varphi)]^{1/2} \tag{21}$$

The third orbital parameter θ is found by recalling the polar equation of an ellipse relative to a coordinate system with center at the focus and with axes coinciding with those of the ellipse. At launch time, the coordinates of the ejected object in this system are R_C, θ, so that one can write

$$R_C = \frac{a(1 - \epsilon^2)}{1 + \epsilon \cos\theta} \tag{22}$$

Equation (20) now is introduced into (22) and the result solved for θ in the form

$$\cos\theta = (\eta/\epsilon)(2 + \eta \cos\varphi) \cos\varphi \tag{23}$$

Equations (21) and (23) reveal that an ejection angle of 0° places the perigee of the object's elliptic orbit at the launch position $\theta = 0°$, whereas a backward launch ($\varphi = 180°$) places the apogee at the launch point $\theta = 180°$. "Upward" and "downward" ejections result in ellipses whose major axes are orthogonal with the line joining the earth's center and the ejection point.

Critical Ejection Angles

A body ejected from a satellite will have the same period of revolution about the earth as does the parent vehicle under the condition that the body's total energy, and hence its total speed, is unchanged by ejection.** The condition is met when the ejection velocity vector makes certain angles, $\pm\varphi_c$, with the satellite orbital velocity vector. These "critical" angles may be found by equating the period for the elliptic orbit, given by $P_E = 2\pi(a^3/\mu)^{1/2}$, and the period for the circular orbit, given by $P_C = 2\pi(R_C^3/\mu)^{1/2}$, and then introducing Eq. (19) to obtain

$$\varphi_c = \cos^{-1}(-\eta/2) \tag{24}$$

Since η is assumed to be small compared with unity, the critical ejection angles that result in closed relative trajectories are seen to be slightly larger than 90° and slightly less than 270°. More generally, an object ejected with speed V_R will follow, in the absence of atmospheric drag, a closed relative trajectory if the ejection velocity vector coincides with any element of a conical surface of semi-angle $\pi - \varphi_c$. This conical surface has its axis aligned with the satellite orbital velocity vector and its apex pointed in the direction of that vector.

If Eq. (24) is inserted in Eq. (19), it is found that at critical ejection the semimajor axis of the elliptic orbit is equal in length to the radius of the satellite's circular orbit.

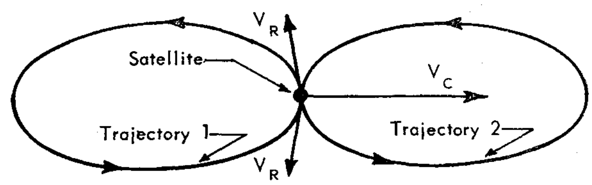

Fig. 2 Illustration of critical angles and elliptical relative trajectories

Relative Trajectories

When ejected at the "upper" critical angle (near 90°), an object follows a relative trajectory having an elliptical shape and lying behind the satellite (trajectory 1 in Fig. 2), whereas ejection at the "lower" critical angle results in an elliptical trajectory that is similar but that lies forward of the satellite rather than behind it (trajectory 2 in Fig. 2). For launch angles in the range $-\varphi_c < \varphi < \varphi_c$, the period of the ejected body in its elliptic orbit is longer than that of the satellite in circular orbit, and the ejected body falls "behind" the satellite; for launch angles outside this range, the ejected body's period is shorter, and it creeps "ahead." With critical-angle ejection, one loop of the trajectory is completed in a time exactly equal to one period of revolution of the satellite (or the object) about the earth; with ejection at any other angle, one loop is completed in approximately one satellite period.

Launched directly forward, i.e., at an angle $\varphi = 0°$, the object follows a trajectory that takes it looping back along the satellite orbit. Over short sections this trajectory closely approximates a prolate cycloid but is better described as resembling a prolate epicycloid. In contrast, a backward ejection at an angle $\varphi = 180°$ yields a trajectory that lies forward of the satellite and that resembles a prolate hypocycloid. If the ejection angle is moved from either of these extremes toward the upper or lower critical angle, the trajectory shape changes smoothly into the closed elliptical form assumed exactly at the critical angle. A launch angle γ lying in the third or fourth quadrant yields a trajectory that is very nearly symmetric (with respect to the origin) to one obtained from a first- or second-quadrant launch angle given by $\varphi = \gamma - \pi$.

The relative trajectories prevailing for zero drag are rather accurately described through an approximate solution of Eqs. (11) and (12) with $B = 0$. If second- and higher-order terms in the coordinates x_3 and y_3 are neglected with respect to R_C, these equations simplify to

$$x_3'' + 2y_3' = 0 \qquad y_3'' - 2x_3' - 3y_3 = 0 \tag{25}$$ ††

This pair of relations readily can be solved to yield, after application of the initial conditions expressed in (13–15),

$$x_3 = -\eta R_C[(3\beta - 4 \sin\beta) \cos\varphi + 2(1 - \cos\beta) \sin\varphi] \tag{26}$$

$$y_3 = \eta R_C[2(1 - \cos\beta) \cos\varphi + \sin\beta \sin\varphi] \tag{27}$$

** This fundamental condition to produce a closed relative trajectory applies whether the satellite is in circular or elliptical orbit and whether the ejection velocity vector lies within or without the satellite orbital plane.

†† Equations equivalent to these were derived in Ref. 11 for the no-drag case.

as the relative coordinates of the launched object corresponding to any launch angle φ. In this case, the symmetry property mentioned previously relating to third- and fourth-quadrant launch angles is exact. Moreover, for ejection angles of 0° and 180°, Eqs. (26) and (27) describe trajectories that are precisely prolate cycloids.

The critical ejection angles need to be redetermined for the present approximate analysis based on (25). This may be done by applying to (26) and (27) the requisite conditions for closed trajectories, namely, $x_3 = y_3 = 0$ for any integral number of satellite revolutions (β any integral multiple of 2π). There results $\varphi_c = \pm \pi/2$.‡‡ To obtain the relative trajectory at critical-angle ejection, φ in (26) and (27) is set equal to $\pm\pi/2$ and the parameter β eliminated from the resulting equations. This gives

$$\frac{(x_3 \pm 2\eta R_C)^2}{(2\eta R_C)^2} + \frac{y_3^2}{(\eta R_C)^2} = 1 \tag{28}$$

which represents a standard ellipse with center at $\pm 2\eta R_C, 0$ in the x_3,y_3 coordinate system and whose major axis is twice the length of its minor axis.

Drift Rate for Near-Critical Launches

Should the actual ejection angle differ from a critical angle by a small amount, the object's relative motion comprises the same elliptical looping found exactly at critical ejection, together with a superimposed "drifting" of the loop center. If the actual ejection angle is slightly less than φ_c, the drift is in the backward direction, whereas if the angle is greater than φ_c, it is forward.

When the satellite has completed one revolution and returned to the point of ejection, a time P_C has elapsed. The additional time for the ejected body in elliptic orbit to reach this point if it is not launched at a critical angle is $P_E - P_C$. For ejection angles close to critical, the speed of the body during this time is very nearly V_C. Hence, the distance M of first closest approach (or first miss distance) of the body and satellite is approximately $M = -V_C(P_E - P_C)$, where a negative value for M signifies that the ejected body passes to the rear of the satellite at closest approach. With $P_E = 2\pi(a^3/\mu)^{1/2}$ and $P_C = 2\pi(R_C^3/\mu)^{1/2}$, one can introduce Eq. (19) to obtain

$$M = V_C P_C[1 - (1 - \eta^2 - 2\eta\cos\varphi)^{-3/2}] \tag{29}$$

Since η has been assumed small, one can apply the binomial expansion and neglect second- and higher-order terms; there results

$$M = -\tfrac{3}{2}\eta^2 V_C P_C[1 + (2/\eta)\cos\varphi] \tag{30}$$

If the actual ejection angle φ differs from a critical angle $\pm\varphi_c$ by the angle δ measured counterclockwise from the critical angle ($\varphi = \pm\varphi_c + \delta$), and if δ is small compared to φ_c, Eq. (30) is approximated by

$$M = \pm 3\eta\delta V_C P_C \tag{31}$$

Dividing both sides of (31) by P_C and replacing η by V_R/V_C leads to a drift rate D of

$$D = \pm 3\delta V_R \tag{32}$$

The quantity D measures the separation rate between the center of the "drifting elliptical loop" and the coordinate origin. As determined in (32), the rate is averaged over the first revolution; however, this initial average rate was found to apply rather accurately for a number of revolutions.

The upper sign in (31) and (32) applies when δ is measured from $+\varphi_c$ and the lower sign when it is measured from $-\varphi_c$. For $\delta > 0$ and measured with respect to the upper critical angle, the ejected object passes ahead of the satellite and both M and D are positive, whereas a positive error angle relative to the lower critical angle leads to a "pass astern" with M and D both negative.

‡‡ As compared with the exact values obtained from (24).

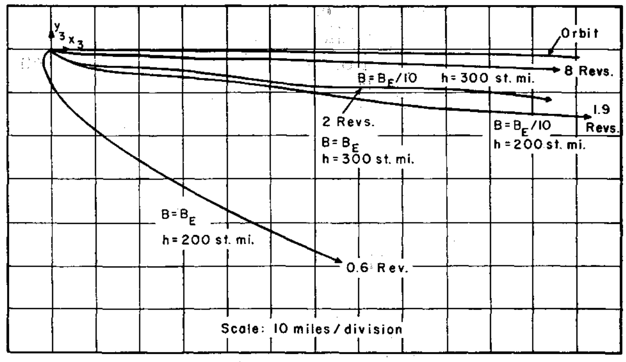

Fig. 3 Trajectories of objects with $B = B_E = 22.5$ ft²/lb and $B = B_E/10$ released with zero ejection speed from a satellite in circular orbit at 200- and 300-miles altitude

General Case: Air Drag Included

An analog computer was used to generate solutions for Eqs. (11) and (12) in the more general case that atmospheric drag force acts on the ejected object (i.e., that $B \neq 0$). Plots of selected typical trajectories obtained in this way are displayed in Figs. 3 and 4. On each plot, the forward direction of orbital motion is to the right, and the x_3,y_3 coordinate system is indicated at the location of the ideal satellite. The satellite orbit also is usually shown. Notation is made at appropriate points of the approximate number of satellite revolutions which have occurred since launch; roughly speaking, each "loop" of a trajectory is equivalent to one revolution. Although the trajectories are relative to an ideal no-drag satellite, they may also be referred to a real satellite, since the latter, if it has a typically low drag parameter, will depart negligibly from the coordinate origin over the time periods of interest. Trajectories are shown for two values of the ballistic drag parameter B: $B_E = 22.5$ ft²/lb, which might apply to a high-drag balloon structure of the sort typified by the Echo satellite, and $B_E/10 = 2.25$ ft²/lb. These high values (typical satellite instrument capsules show B's on the range

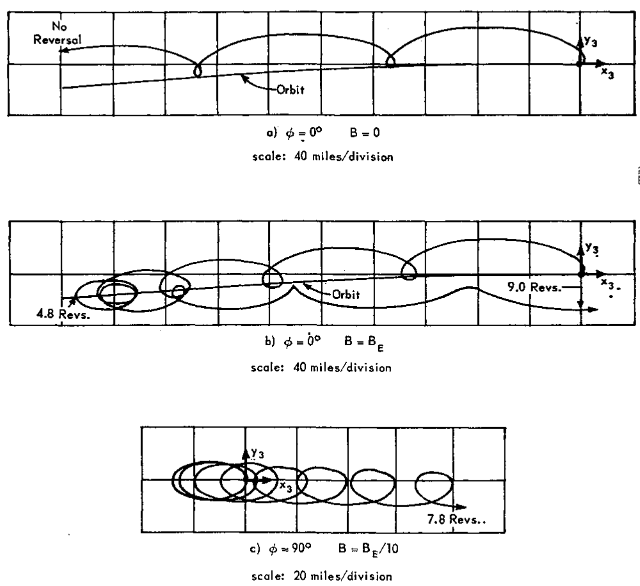

Fig. 4 Trajectories of objects ejected with a speed of 29 mph from a satellite in circular orbit at 300-miles altitude: a) $B = 0$ (equivalent to no-drag condition), $\varphi = 0°$; b) $B = B_E = 22.5$ ft²/lb, $\varphi = 0°$; c) $B = B_E/10$, $\varphi = 90°$

0.01 to 0.1 ft²/lb) were chosen to shorten computer runs and hence improve accuracy while displaying trajectory form well. All trajectories are based on an air-density vs altitude curve fitted to data of Nicolet[12] and Kallman[13]; this curve§§ gives values of 3.5×10^{-14} and 2.2×10^{-15} g/cm³, respectively, at the two ejection altitudes of 200 and 300 statute miles represented by Figs. 3 and 4.

Nature of the Trajectories

Without air drag acting, the case of release (i.e., zero ejection speed) is trivial. With air drag acting, however, the released object undergoes an added acceleration that is, in general, directed forward and slightly downward. Thus, after initial transient behavior, it follows a spiral descent path about the earth.

Figure 3 depicts the relative trajectories of objects having drag parameters of B_E and $B_E/10$ released with zero ejection speed from a satellite in circular orbit at altitudes of 200 and 300 statute miles. Two details of the motion are of especial interest. The first is an initial hook on the trajectory, here most obviously displayed on the curve for $B = B_E$ and altitude = 200 miles. An elementary analysis of the behavior immediately after release confirms one's "intuitive" feeling that the object undergoing drag first must move directly rearward under the effect of the "wind." Only as orbital velocity is lost does the object begin to drop in altitude. Ultimately, of course, conversion of potential energy into kinetic form as altitude is reduced gives a forward component of velocity which carries the object past the no-drag satellite and thus generates the hook. The second feature shown by the curves is a damped sinusoidal oscillation of small amplitude which is seen superimposed on the otherwise smooth trajectories. Here this is displayed most clearly on the curves for $B = B_E/10$ and altitude = 200 miles and for $B = B_E$ and altitude = 300 miles. This oscillation, together with the hook, probably constitutes a transient response to the "step-function" shock excitation of the system represented by the sudden application of drag force. Presumably a similar transient response follows the cessation of drive force when a satellite is placed in orbit.

Figure 4 displays three trajectories for objects ejected at an altitude of 300 miles; in each case the ejection speed is approximately 29 mph, corresponding to $\eta = \frac{1}{600}$. Figure 4a shows the trajectory shape for zero drag and forward ejection ($\varphi = 0°$), very nearly a prolate epicycloid, as discussed earlier. Figure 4b shows what happens to that trajectory when air drag is added. The initial part of the trajectory closely resembles the zero-drag case in Fig. 4a, but as time progresses the effect of air drag is more and more noticeable in shifting the curve forward and slightly downward from its corresponding zero-drag position. Eventually, the overall retrograde motion ceases at a distance of about 350 to 400 miles behind the satellite, and the object seems to "pause" and make several loops in the same region before starting a forward motion that carries it ahead of and below the satellite. Figure 4c shows the trajectory for a near-critical upward shot ($\varphi = 90°$) with $B = B_E/10$ at 300-miles altitude. It is recalled that the near-critical launch without air drag leads to relative motion describable as an elliptical looping with a superimposed drift motion of the loop center. Now, with air drag acting, still another drift motion is superimposed which accelerates the center of the loop forward and slightly downward and tends to dampen the looping. Not illustrated are trajectories for $\varphi = 270°$, which would closely resemble that for $\varphi = 90°$ except with the initial loop lying forward instead of behind, and for $\varphi = 180°$, which would give approximately a prolate hypocycloid ahead of the satellite combined with the superimposed forward and slightly downward accelerative tendency due to air drag.

§§ Recent values of air density published by Kallmann-Bijl[14] indicate that the curve lies within the daytime-to-nighttime density range over the altitudes of interest here.

Effect of Parameter Variation

In general, varying the ejection angle φ causes a smooth change in trajectory shape. Thus, for example, as φ is increased from zero, the long rearward excursion that occurs for forward launch (Fig. 4b) gradually shortens until at 90° the trajectory becomes the moving elliptical loop already noted (Fig. 4c).

Increasing ejection speed V_R enlarges the size of the trajectory loops in roughly direct proportion; i.e., doubling V_R doubles loop size. Increasing V_R tends to increase the time spent by the object in the satellite's general vicinity, though not in direct proportion. For forward shots displaying the retrogression illustrated in Fig. 4b, the distance of maximum retrogression at a specified ejection angle increases almost proportionately with V_R.

Either decreasing B or increasing altitude reduces air-drag effects and changes trajectory shape in a fashion that is qualitatively predictable. At 300-miles altitude, for example, a tenfold decrease in B for a launch at $\varphi = 0°$ lengthens the retrogression distance shown in Fig. 4b by a factor of about 8. With B fixed at B_E, decreasing the altitude from 300 to 200 miles (which raises air density slightly more than tenfold) changes the long rearward excursion of Fig. 4b into a single partial loop shaped like a reversed comma and terminating in a fast dive to earth. The latter trajectory shape is typical of objects having the high drag parameter $B = B_E$ when ejected at 200-miles altitude, regardless of ejection speed and angle. Bodies having $B = B_E/10$ ejected at 200-miles altitude may undergo a few loops before diving, provided the ejection direction is well forward and/or the ejection speed is significant.

Pause Tendency

It is well known that, in general, the decay of an initially elliptical orbit proceeds somewhat as follows. At first, the apogee drops faster than does the perigee, so that orbital eccentricity decreases until the orbit is roughly circular. Thereafter, the path of the descending body is a spiral that gradually tightens about the earth. The trajectories discussed herein elucidate these changes for the case of slight initial eccentricity. Of particular interest is the pause, illustrated in Fig. 4b, which can be identified with the transition from decaying ellipse to spiral trajectory.

Examination of Fig. 4b discloses that, prior to the pause, both the orbital perigee (bottoms of trajectory loops) and the apogee (tops of loops) are dropping, but the apogee is dropping faster. At the time of pause, the original asymmetry of the trajectory loops has disappeared and the loops are approximately elliptical in form, corresponding to those that prevail initially after a near-critical ejection; moreover, at pause the loops are centered approximately at the altitude of the satellite orbit. After pause, the loops again become asymmetrical and gradually dampen out to give a smooth trajectory representing the spiral phase of the descent. A simple energy analysis further clarifies these changes and enables the approximate time between ejection and pause to be predicted.

At the time of pause, the body is executing elliptical loops of approximately the same size, shape, and altitude as would have prevailed immediately after critical-angle ejection. From this it may be concluded that the body's total energy at the time of pause is about the same as it would have been after critical launch. As noted earlier, critical ejection signifies that the body's total energy is unchanged by ejection. Thus, at pause the body's total energy is approximately the same as before launch, a fact that establishes the significance of the pause. The body receives an additional energy $(\Delta E)_E$ from a forward ejection; thereafter, the body's total energy is dissipated by air drag until, at the time of pause, the total energy has been returned to its pre-ejection value. Hence, the ejection-to-pause time for a launch in the forward direction is the time required for air drag to dissipate the additional energy imparted by ejection.

The change $(\Delta E)_E$ in the body's total energy caused by its impulsive ejection from the satellite is found with the aid of Eq. (17):

$$(\Delta E)_E = (m/2)V_E^2[1 + (2/\eta)\cos\varphi] \tag{33}$$

This expression shows the energy change to be zero for ejection at the critical angles $\pm\varphi_c$ found from (24) and to be maximum at $\varphi = 0°$. A satellite body will lose energy to air resistance at a rate that is the product of drag force and speed; in terms of the drag parameter B, this rate is $mB\rho V^3$. For a not-too-long time t, such that air density ρ and speed V have not changed much from their initial values, the energy lost in overcoming drag is approximately

$$(\Delta E)_D = mB\rho V_C^3 t \tag{34}$$

where the speed is written as V_C, the satellite orbital speed, and the air density ρ is that for the nominal altitude of the launching satellite. Equating (34) with (33) and solving for t yields, for the approximate ejection-to-pause time,

$$t = (\eta^2/2B\rho V_C)[1 + (2/\eta)\cos\varphi] \tag{35}$$

Equation (35) has been checked against many trajectories and found to agree, in all cases where a distinct pause takes place, within the uncertainty with which a pause time can be measured. When t falls below about 45 to 60 min, a distinct pause does not take place and the energy-decay time from Eq. (35) has no apparent significance to the trajectory form obtained. No pause occurs when the initial energy imparted by ejection is small (as for ejection angles near 90°) or when the rate of energy dissipation due to air drag is large (as for low altitude and/or large B).

It is noteworthy that the ejected body appears never to achieve a perfectly circular orbit at the time of pause, but only a near-circular one. Of numerous trajectories displaying pause for ejection angles from 0° to near 90°, all show at pause elliptical loops centered approximately on the satellite orbit. Thus, although in general an initially elliptical orbit about the earth decays quite close to a circular form, it seems never actually to transform into a circular orbit at the transition; oscillations in altitude of an orbital body persist until the spiral phase of the descent path clearly is underway.

References

[1] Hord, R. A., "Relative motion in the terminal phase of interception of a satellite or a ballistic missile," NACA TN 4399 (September 1958).

[2] Brunk, W. E. and Flaherty, R. J., "Methods and velocity requirements for the rendezvous of satellites in circumplanetary orbits," NASA TN D-81 (October 1959).

[3] Spradlin, L. W., "The long-time satellite rendezvous trajectory," *IAS National Specialist Meeting on Guidance of Aerospace Vehicles* (Inst. Aerospace Sci., New York, 1960), pp. 21–24.

[4] Spradlin, L. W., "The long-time satellite rendezvous trajectory," Aero/Space Eng. **19**, 32–37 (1960).

[5] Eggleston, J. M., "Optimum time to rendezvous," ARS J. **30**, 1089–1091 (1960).

[6] Eggleston, J. M. and Beck, H. D., "A study of the positions and velocities of a space station and a ferry vehicle during rendezvous and return," NASA TR R-87 (1961).

[7] Eggleston, J. M., "A study of the optimum velocity change to intercept and rendezvous," NASA TN D-1029 (February 1962).

[8] Soule, P. W., "Rendezvous with satellites in elliptical orbits with low eccentricity," *Advances in the Astronautical Sciences* (Macmillan Co., New York, 1961), Vol. 7, pp. 138–147.

[9] Perry, W. R., "Rendezvous compatible orbits," NASA Rept. MTP-M-S&M-F-61-2 (1961).

[10] Liebermann, S. I., "Rendezvous acceptability regions based on energy considerations," ARS J. **32**, 287–290 (1962).

[11] White, W., "Electromagnetic analogs for the gravitational fields in the vicinity of a satellite," Proc. Inst. Radio Engrs. **46**, 920–922 (1958).

[12] Nicolet, M., "The constitution and composition of the upper atmosphere," Proc. Inst. Radio Engrs. **47**, 142–147 (1959).

[13] Kallmann, H., "A preliminary model atmosphere based on rocket and satellite data," J. Geophys. Research **64**, 615–623 (1959).

[14] Kallmann-Bijl, H., "Daytime and nighttime atmospheric properties derived from rocket and satellite observations," J. Geophys. Research **66**, 787–795 (1961).